

# Infrared Spectra of the H<sub>2</sub>S- -HF and H<sub>2</sub>Se- -HF Hydrogen-Bonded Complexes in Solid Argon

ROBERT T. ARLINGHAUS and LESTER ANDREWS\*

Received September 6, 1984

Several hydrogen bonded complexes of H<sub>2</sub>S + HF and H<sub>2</sub>Se + HF have been prepared by condensing the argon-diluted reagents at 12 K. Strong  $\nu_s(\text{H-F})$  stretching modes were observed at 3652 and 3655 cm<sup>-1</sup> for the 1:1 H<sub>2</sub>S- -HF and H<sub>2</sub>Se- -HF complexes, respectively, suggesting comparable hydrogen-bond strengths. The observation of two  $\nu_l(\text{H-F})$  librational modes is consistent with pyramidal structures for the complexes. A stable reverse complex HF- -HSH is characterized by a single  $\nu(\text{H-F})$  absorption at 3799 cm<sup>-1</sup>, and a H<sub>2</sub>S- -(HF)<sub>2</sub> complex is characterized by  $\nu(\text{H}_b\text{-F})$  and  $\nu(\text{H}_a\text{-F})$  modes above and below the single  $\nu_s(\text{H-F})$  mode of the H<sub>2</sub>S- -HF complex. Several other 2:1 and 1:2 base + HF complexes have been identified by strong absorptions in the HF stretching region.

## Introduction

The H<sub>2</sub>O- -HF and H<sub>2</sub>S- -HF heterodimers are of interest in the study of hydrogen bonding because of the difference in valence angles and hybridization in the base monomers ( $\angle\text{HOH} = 105^\circ$  and  $\angle\text{HSH} = 92^\circ$ ).<sup>1</sup> The H<sub>2</sub>O- -HF complex has been studied in the gas phase by infrared and microwave spectroscopy<sup>2-4</sup> and in an argon matrix by infrared spectroscopy.<sup>5</sup> The microwave studies have established a pyramidal structure for the complex with a  $46 \pm 8^\circ$  angle between the HOH mirror plane and HF axis and a low barrier to inversion. Matrix infrared spectra of hydrogen-bonded complexes provide complementary information to the microwave studies. The matrix spectrum of the H<sub>2</sub>O + HF complex revealed a strong, sharp  $\nu_s(\text{H-F stretch})$  absorption at 3554 cm<sup>-1</sup> and a pair of  $\nu_l(\text{H-F libration})$  quartets beginning at 753 and 636 cm<sup>-1</sup>, which characterize a strong pyramidal complex with librational modes split by inversion doubling.

The second-row base H<sub>2</sub>S- -HF complex has been identified in two microwave studies, and a right-angle pyramidal structure has been established.<sup>6,7</sup> Complementary argon matrix infrared spectra have been recorded for H<sub>2</sub>S- -HF and the third-row base H<sub>2</sub>Se- -HF complex, and the results will be described below.

## Experimental Section

The apparatus and techniques have been described previously.<sup>8,9</sup> Spectra were recorded on a Nicolet 7199 Fourier transform infrared (FTIR) spectrometer between 4000 and 400 cm<sup>-1</sup> at 1-cm<sup>-1</sup> resolution with  $\pm 0.3\text{-cm}^{-1}$  accuracy. Spectra for several DF experiments were recorded to the nearest wavenumber on a Beckman IR-12 grating spectrometer between 4000 and 200 cm<sup>-1</sup> in order to observe lower frequency librational modes.

Hydrogen fluoride and hydrogen sulfide (Matheson) were frozen at 77 K and evacuated to remove volatile impurities and then expanded into well-passivated stainless-steel cans. The preparation of deuterium fluoride has been described elsewhere.<sup>8</sup> Hydrogen selenide was synthesized by dripping a 30% HCl solution onto a finely divided sample of ZnSe (Aldrich); the vapor produced was dried on CaCl<sub>2</sub> and purified by condensation and vacuum distillation at 77 K. Deuterium sulfide was prepared by condensing H<sub>2</sub>S on 2 mL of D<sub>2</sub>O in a Pyrex tube and allowing exchange for 24 h. The D<sub>2</sub>S samples (approximately 10% H<sub>2</sub>S, 30% HDS, and 60% D<sub>2</sub>S as observed from  $\nu_s$  intensities) were condensed at 77 K, evacuated, and expanded into a deuterated stainless-steel can. Deuterium selenide (10% H<sub>2</sub>Se, 30% HDS<sub>e</sub>, 60% D<sub>2</sub>Se) was prepared in a similar manner.

The samples were diluted with argon to Ar/reagent = 100/1 to 1000/1 mixtures. The base and acid argon mixtures were simultaneously

condensed onto a 9-12 K CsI window at 2-5 mmol/h rates for up to 20 h, and a spectrum was recorded. The samples were annealed several times between 16 and 26 K for 10 min and re-cooled, and spectra were recorded after each warming cycle to monitor the diffusion and association of molecular species.

## Results

A total of 21 experiments were performed with hydrogen sulfide, selenide, and fluoride and the deuterated acids. The following results are representative of the data collected in several experiments.

**H<sub>2</sub>S + HF.** A matrix was formed by codeposition of 30 mmol from each of Ar/H<sub>2</sub>S = 400/1 and Ar/HF = 200/1 samples. After deposition an FTIR spectrum was recorded and compared to matrix spectra of separate H<sub>2</sub>S and HF samples. This spectrum, shown in Figure 1a, revealed several new product absorptions: a weak absorption at 3799 cm<sup>-1</sup> labeled R ( $A = \text{absorbance unit} = 0.03$ ), a strong sharp band labeled  $\nu_s$  at 3652 ( $A = 0.70$ ), a weak band at 870 cm<sup>-1</sup> labeled  $2\nu_l$ , a band at 508 cm<sup>-1</sup> with a 498-cm<sup>-1</sup> shoulder, and an absorption at 481 cm<sup>-1</sup> ( $A = 0.05$ ) with a weaker satellite at 486 cm<sup>-1</sup> (labeled  $\nu_l$ ). The bands labeled N, D, W, and T are present in HF experiments and are due to N<sub>2</sub>- -HF, (HF)<sub>2</sub>, H<sub>2</sub>O, and (HF)<sub>3</sub>, respectively.<sup>10</sup> The matrix was annealed to 16 K for 10 min and re-cooled to 9 K; the  $\nu_s$  and  $\nu_l$  bands increased by one-third, and the R band was unchanged. Finally the sample was annealed to 24 K, and the resulting spectrum is shown in Figure 1b. The  $\nu$  bands observed on deposition tripled in intensity, the R band increased 5-fold, and several new absorptions were observed at 3714 ( $A = 0.13$ ) and 3563 ( $A = 0.40$ ) labeled 3, at 3513 ( $A = 0.07$ ), and at 3489, 3380, 3282, and 3150 cm<sup>-1</sup>. In the low-frequency region new absorptions labeled 3 were observed at 554, 534, 468, and 457 cm<sup>-1</sup>. Several experiments with Ar/H<sub>2</sub>S concentrations of between 100/1 to 200/1 were performed. The absorptions with labels  $\nu_s$ ,  $\nu_l$ , and  $2\nu_l$  were observed with the same relative intensities as observed in the experiment just described. The groups of absorptions with labels R and 3 were also observed with constant relative intensities. The band at 3515 cm<sup>-1</sup> was much more intense in the more concentrated experiments. Several weak bands not observed in the less concentrated experiments were seen at 575 ( $A = 0.027$ ), 599, and 604 cm<sup>-1</sup>. The absorptions observed in the H<sub>2</sub>S + HF experiments are collected in Table I.

**H<sub>2</sub>S + DF.** Argon-diluted H<sub>2</sub>S was codeposited with a 70% DF-enriched mixture; the DF stretching region was complicated by the presence of H<sub>2</sub>S monomer and polymer stretching absorptions. The more intense bands observed in the HF experiments were again present, and several new product absorptions specific to DF were observed at 2831, 2729, 2688 ( $A = 1.0$ ), and 2632 cm<sup>-1</sup>. The matrix was annealed to 24 K, and the spectrum is shown in Figure 2a; the strong absorption labeled  $\nu_s$  at 2688 cm<sup>-1</sup> increased only slightly in intensity. The band at 2831 cm<sup>-1</sup> labeled R approximately doubled while the two bands labeled 3 at 2729 and 2632 cm<sup>-1</sup> ( $A = 0.60$ ) increased 6-fold.

- (1) Sutton, L. E., Ed. *Spec. Publ.—Chem. Soc.* 1958, No. 11.
- (2) Thomas, R. K. *Proc. R. Soc. London, Ser. A* 1975, 344, 579.
- (3) Bevan, J. W.; Kisiel, Z.; Legon, A. C.; Millen, D. J.; Rogers, S. C. *Proc. R. Soc. London, Ser. A* 1980, 372, 441.
- (4) Kisiel, Z.; Legon, A. C.; Millen, D. H. *Proc. R. Soc., London Ser. A* 1982, 381, 419.
- (5) Andrews, L.; Johnson, G. L. *J. Chem. Phys.* 1983, 79, 3670.
- (6) Visawanathan, R.; Dyhr, T. R. *J. Chem. Phys.* 1982, 77, 1166.
- (7) Willoughby, L. C.; Fillery-Travis, A. J.; Legon, A. C. *J. Chem. Phys.* 1984, 81, 20.
- (8) Johnson, G. L.; Andrews, L. *J. Am. Chem. Soc.* 1982, 104, 3043.
- (9) Andrews, L.; Johnson, G. L. *J. Chem. Phys.* 1982, 76, 2875.

- (10) Andrews, L.; Johnson, G. L. *J. Phys. Chem.* 1984, 88, 425.

Table I. Cocondensation Product Absorptions ( $\text{cm}^{-1}$ ) for Hydrogen or Deuterium Sulfide and HF or DF Hydrogen-Bonded Complexes

$\text{H}_2\text{S} + \text{HF}$	$\text{D}_2\text{S} + \text{HF}$	$\text{H}_2\text{S} + \text{DF}$	$\text{D}_2\text{S} + \text{DF}$	assgmt
3799	3791	2831	2822	$\nu(\text{H-F})$ , 2
3714	3713	2729		$\nu(\text{H}_b\text{-F})$ , 3
3652	3646	2688	2684	$\nu_s$ , 1
3563	3556	2632	2627	$\nu(\text{H}_a\text{-F})$ , 3
3513	3503			$\nu(\text{H-F})$ , $(\text{H}_2\text{S})(\text{HF})(\text{H}_2\text{S})$
3489	3480			$\nu(\text{H-F})$ , $(\text{H}_2\text{S})(\text{HF})_x$
3425				$\nu(\text{H-F})$ , $(\text{H}_2\text{S})(\text{HF})_x$
3380	3374			$\nu(\text{H-F})$ , $(\text{H}_2\text{S})(\text{HF})_x$
3282	3272			$\nu(\text{H-F})$ , $(\text{H}_2\text{S})(\text{HF})_x$
3150	3140			$\nu(\text{H-F})$ , $(\text{H}_2\text{S})(\text{HF})_x$
870	856			$2\nu_1$ , 1
604	593			$\nu(\text{H-F})$ , $(\text{H}_2\text{S})(\text{HF})_x$
599	588			$\nu(\text{H-F})$ , $(\text{H}_2\text{S})(\text{HF})_x$
575	575			$\nu(\text{H-F})$ , $(\text{H}_2\text{S})(\text{HF})_x$
554, 534	526			$\nu_1(\text{H}_a\text{-F})$ , 3
508, 481	496, 475	406, 377	381, 363	$\nu_1$ , 1
468, 457	460			$\nu_1(\text{H}_b\text{-F})$ , 3

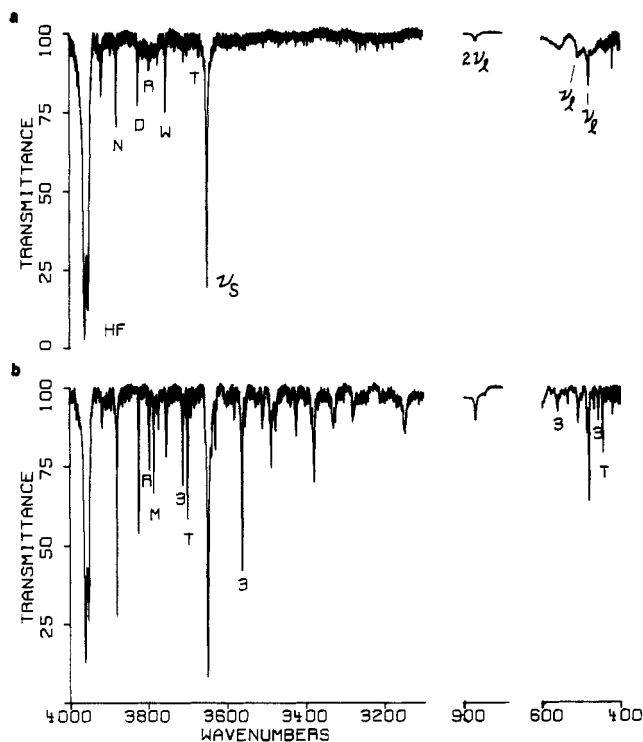


Figure 1. Fourier transform infrared spectra of  $\text{Ar}/\text{H}_2\text{S} = 400/1$  and  $\text{Ar}/\text{HF} = 200/1$  samples: (a) after cocondensation at 12 K; (b) after annealing to 24 K for 10 min and recooling to 12 K. Peaks: N =  $\text{N}_2$ -HF, D =  $(\text{HF})_2$ , M =  $\text{N}_2$ - $(\text{HF})_2$ , W =  $\text{H}_2\text{O}$ , T =  $(\text{HF})_3$ .

A matrix was prepared with 50% DF to study the low-frequency region, and the spectrum is shown in Figure 2b. The bands specific to HF at  $508 \text{ cm}^{-1}$  with a weaker satellite at  $500 \text{ cm}^{-1}$  and the more intense absorptions at  $481 \text{ cm}^{-1}$  ( $A = 0.48$ ) with a satellite at  $486 \text{ cm}^{-1}$  were again observed; a similar group of absorptions was observed at  $407 \text{ cm}^{-1}$  with a weaker satellite at  $400 \text{ cm}^{-1}$  and at  $378 \text{ cm}^{-1}$  with a weaker shoulder at  $384 \text{ cm}^{-1}$ . The  $\text{H}_2\text{S}$ -DF absorptions are listed in Table I.

**$\text{D}_2\text{S} + \text{HF}$  and DF.** Similar experiments were performed with  $\text{D}_2\text{S}$  and HF; the spectrum from a sample prepared with  $\text{Ar}/\text{D}_2\text{S} = 150/1$  and  $\text{Ar}/\text{HF} = 300/1$  mixtures is shown in Figure 3. Three partially resolved bands were observed at  $3652$ ,  $3648$ , and  $3646 \text{ cm}^{-1}$  under high resolution; the dominant  $3646\text{-cm}^{-1}$  band ( $A = 1.0$ ) is labeled  $\nu_s$  in the figure. Several other new product absorptions were observed at  $3791 \text{ cm}^{-1}$  labeled R, at  $3713$  and  $3556 \text{ cm}^{-1}$  labeled 3, and at  $856 \text{ cm}^{-1}$  labeled  $2\nu_1$ , and a pair of absorptions at  $496$  ( $A = 0.14$ ) and  $475 \text{ cm}^{-1}$  ( $A = 0.26$ ) labeled  $\nu_1$ , were also observed. The matrix was annealed to 26 K, and a spectrum revealed a 5% increase for the  $\nu_s$ ,  $\nu_1$ , and  $2\nu_1$  absorptions, a 2-fold increase in the  $3791\text{-cm}^{-1}$  (R) absorption, and a 5-fold increase in the  $3713\text{-}$  and  $3556\text{-cm}^{-1}$  bands (3). This warm-up

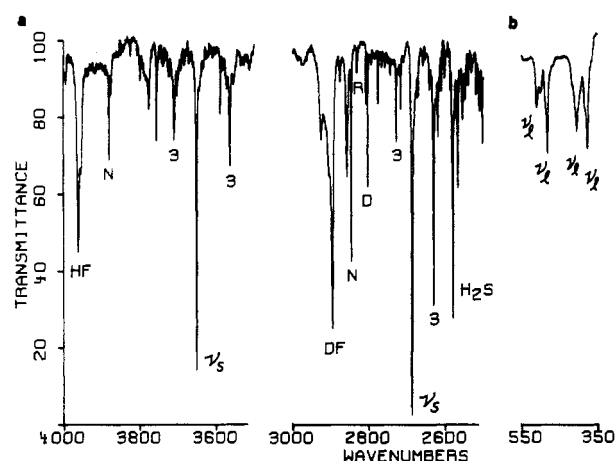


Figure 2. (a) Fourier transform infrared spectrum of  $\text{Ar}/\text{H}_2\text{S} = 300/1$  and  $\text{Ar}/(\text{DF} + \text{HF})$  samples after annealing to 21 K for 10 min and recooling to 12 K. (b) Grating infrared spectra of similar samples deposited at 15 K.

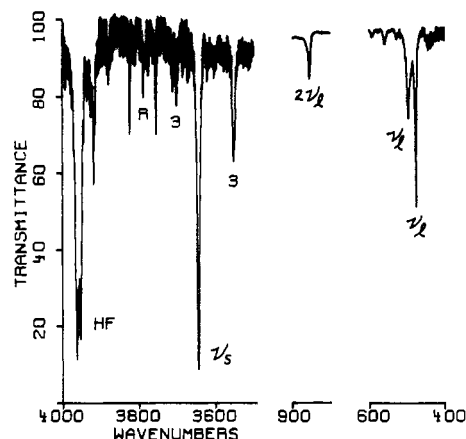
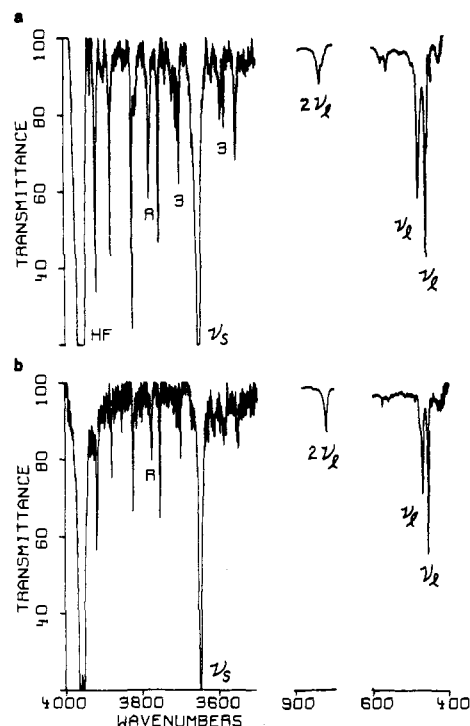


Figure 3. FTIR spectrum of  $\text{Ar}/\text{D}_2\text{S} (=150/1) + \text{Ar}/\text{HF} (=300/1)$  samples after cocondensation at 12 K.

also produced several new product absorptions similar to those observed from  $3100$  to  $3500 \text{ cm}^{-1}$  in the  $\text{H}_2\text{S} + \text{HF}$  experiments. Other samples were prepared with DF + HF mixtures, and the results are collected in Table I.

**$\text{H}_2\text{Se} + \text{HF}$  and DF.** The spectrum of a matrix formed by codepositing argon-diluted samples of  $\text{H}_2\text{Se}$  and HF is shown in Figure 4a. New product absorptions not observed in matrix  $\text{H}_2\text{Se}$  or HF spectra include a completely absorbing band labeled  $\nu_s$  at  $3655 \text{ cm}^{-1}$ , an absorption at  $3787 \text{ cm}^{-1}$  ( $A = 0.23$ ) labeled R, and two weak absorptions labeled 3 at  $3719$  and  $3595 \text{ cm}^{-1}$ . In the low-frequency region new absorptions were observed at  $834 \text{ cm}^{-1}$  ( $A = 0.04$ ) labeled  $2\nu_1$  and a doublet labeled  $\nu_1$  at  $461$  and  $479$



**Figure 4.** FTIR spectra: (a) Ar/H<sub>2</sub>Se = 200/1 and Ar/HF samples after cocondensation at 12 K; (b) Ar/D<sub>2</sub>Se = 200/1 and Ar/HF samples after cocondensation at 12 K.

**Table II.** Cocondensation Product Absorptions (cm<sup>-1</sup>) for H<sub>2</sub>Se or D<sub>2</sub>Se and HF or DF Hydrogen-Bonded Complexes in Solid Argon

H <sub>2</sub> Se + HF	D <sub>2</sub> Se + HF	H <sub>2</sub> Se + DF	assgnt
3783	3779	2811	$\nu(\text{H-F})$ , HF--HSeH
3719	3718	2731	$\nu(\text{H}_b\text{-F})$ , 1:2 <sup>a</sup>
3655	3651	2691	$\nu_s$
3595	3590	2650	$\nu(\text{H}_a\text{-F})$ , 1:2 <sup>a</sup>
3499	3492		$\nu(\text{H-F})$ , 2:1 <sup>b</sup>
3311	3308		$\nu(\text{H-F})^c$
3192	3188		$\nu(\text{H-F})^c$
834	820		$2\nu_1$
479, 461	471, 456	381, 359	$\nu_1$

<sup>a</sup> H<sub>2</sub>Se--H<sub>a</sub>-F--H<sub>b</sub>-F complex like 3. <sup>b</sup> H<sub>2</sub>Se--H-F--HSeH complex. <sup>c</sup> Higher order (H<sub>2</sub>Se)(HF)<sub>x</sub> complex.

cm<sup>-1</sup>. Annealing the matrix to 24 K produced a 10% increase in the above bands, a 2-fold growth in the R absorption, and a 6-fold growth in the bands labeled 3. Experiments with DF and H<sub>2</sub>Se gave DF counterparts for the above product bands, which are collected in Table II.

A spectrum of a matrix prepared with D<sub>2</sub>Se + HF is shown in Figure 4b. Important new product absorptions were observed at 3651 cm<sup>-1</sup> (completely absorbing, labeled  $\nu_s$ ), at 3777 cm<sup>-1</sup> labeled R, at 3718 and 3589 cm<sup>-1</sup> labeled 3, and at 821 cm<sup>-1</sup> ( $2\nu_1$ ), and a doublet labeled  $\nu_1$  was also observed at 455 ( $A = 0.35$ ) and 470 cm<sup>-1</sup>. The matrix was annealed, and growth in the aforementioned absorptions and production of new product species were similar to that observed in the H<sub>2</sub>Se + HF experiment. Results from all selenide experiments are listed in Table II.

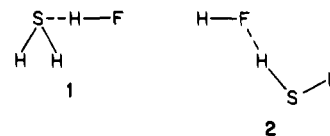
### Discussion

The products of the H<sub>2</sub>S and H<sub>2</sub>Se + HF cocondensation reactions will be identified, assignments will be made, and spectral information on bonding and structure in the product complexes will be discussed.

**Identification.** The new product absorptions listed in Tables I and II were not observed in argon matrix samples of hydrogen sulfide, hydrogen selenide, or hydrogen fluoride; these bands were produced with high yields when the reagents were mixed during condensation and when the matrices were annealed. The product

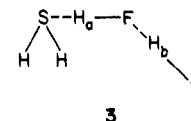
bands can be separated into several groups on the basis of concentration studies and sample annealing.

The strong  $\nu_s$  band in the high-frequency region and weaker bands  $2\nu_1$  and  $\nu_1$  bands in the low-frequency region are the major product absorptions for the H<sub>2</sub>S + HF cocondensation reaction. These bands were produced with the largest yields upon reagent deposition and increased on annealing the more dilute samples but decreased slightly on warming the more concentrated samples. This behavior is appropriate for a 1:1 complex. The  $\nu_s$  band is due to an H-F stretching fundamental, as revealed from the large DF shift, and small displacements in the  $\nu_s$  and  $\nu_1$  bands on D<sub>2</sub>S substitution show that H<sub>2</sub>S is also involved in the complex. The  $2\nu_1$  and  $\nu_1$  absorptions display constant intensities relative to the  $\nu_s$  band upon sample annealing, which indicates that they are also associated with the major product species 1.



The weak sharp band labeled R at 3799 cm<sup>-1</sup> was observed in all experiments upon reagent condensation and increased slightly on sample annealing, which is also consistent with a 1:1 complex. The large DF shifts and small shifts with D<sub>2</sub>S indicate an H-F stretching fundamental and the involvement of H<sub>2</sub>S in the complex. The substantially smaller displacement of this band from the HF fundamental<sup>10</sup> at 3919 cm<sup>-1</sup> relative to the  $\nu_s(\text{H-F})$  absorption suggests a different type of complex 2. Such a reverse complex has been observed previously in H<sub>2</sub>O + HF and HCN + HF cocondensation reactions.<sup>4,11</sup>

The product absorptions labeled 3 appeared in dilute experiments after reagent condensation and increased markedly with constant relative intensities upon sample warming. One of the product bands is displaced more and one displaced less than the single  $\nu_s(\text{H-F})$  mode of product species 1. This indicates one stronger and one weaker H-F bond in the higher order complex as found for the analogous H<sub>2</sub>O--HF and H<sub>2</sub>O--(HF)<sub>2</sub> complexes.<sup>4</sup> These bands are therefore identified as the 1:2 H<sub>2</sub>S--(HF)<sub>2</sub> complex 3.



The 3513-cm<sup>-1</sup> absorption was weak in dilute H<sub>2</sub>S experiments and very strong in concentrated experiments, which indicates that more than one H<sub>2</sub>S molecule is involved in the complex. This band was the only product that showed a higher order dependence on H<sub>2</sub>S concentration. The observation of a single absorption in the H-F stretching region displaced substantially more than the single  $\nu_s$  band of the 1:1 complex indicates one weaker H-F bond in this complex. The 3513-cm<sup>-1</sup> absorption is therefore assigned to the 2:1 complex H<sub>2</sub>S--HF--HSH with the HF submolecule in the middle position.

The sharp product absorptions between 3100 and 3500 cm<sup>-1</sup> in Table I were only observed after sample warming and decreased in intensity in more dilute HF experiments. These absorptions are most likely due to 1:2 and 1:3 (H<sub>2</sub>S)(HF)<sub>x</sub> reaction products where the H<sub>2</sub>S and HF molecules may act as both an acid and a base.

**H<sub>2</sub>S + HF Assignments.** The strong, sharp 3652-cm<sup>-1</sup> absorption is assigned to the  $\nu_s(\text{H-F})$  stretching fundamental in complex 1 based on the near agreement of the HF/DF = 3652/2688 = 1.359 ratio with the 3919/2876 = 1.363 ratio for the diatomic molecule in solid argon<sup>10</sup> and the small red-shifts to 3648 and 3646 cm<sup>-1</sup> for the HDS--HF and D<sub>2</sub>S--HF complexes, respectively. The low-frequency doublet with a strong component at 481 cm<sup>-1</sup> and a weaker component at 508 cm<sup>-1</sup> is

(11) Johnson, G. L.; Andrews, L. J. *Am. Chem. Soc.* 1983, 105, 163.

assigned to the two H-F librational modes,  $\nu_1$ , one in the plane bisecting the H<sub>2</sub>S bond angle and the other perpendicular to this plane. The two weak satellite bands at 498 and 486 cm<sup>-1</sup> are presumably due to matrix site splittings. The observation of two different librational modes with different  $\nu_1(\text{HF})/\nu_1(\text{DF})$  ratios of 508/406 = 1.251 and 481/377 = 1.276 is consistent with the pyramidal structure determined from the microwave spectrum, which requires asymmetry in the librational potential function. A similar asymmetry was observed for H<sub>2</sub>O-HF, which exhibited a larger separation between the  $\nu_1$  modes. The small displacements in both  $\nu_1$  modes with D<sub>2</sub>S substitution and the different 496/380 = 1.305 and 475/363 = 1.308 ratios suggest minor coupling between  $\nu_1$  and the lower frequency bending mode of the complex. The weak broader absorption at 870 cm<sup>-1</sup> is assigned to a librational overtone  $2\nu_1$  based on the large red-shift to 856 cm<sup>-1</sup> for D<sub>2</sub>S-HF. This is probably the overtone for the stronger librational mode at 481 cm<sup>-1</sup> with the other overtone too weak to observe in our experiments. In experiments with (CH<sub>3</sub>)<sub>2</sub>S + HF a strong librational mode doublet with one strong and one weak component was observed along with strong and weak overtone components.<sup>12</sup> The low  $\nu_1(\text{HF})/\nu_1(\text{DF})$  ratios and the  $2\nu_1/\nu_1$  ratios of 1.809 and 1.802 for H<sub>2</sub>S-HF and D<sub>2</sub>S-HF indicate anharmonicity in the librational potential function. No base submolecule modes were observed for the H<sub>2</sub>S-HF complex owing to the complicated matrix spectrum for H<sub>2</sub>S and (H<sub>2</sub>S)<sub>n</sub> species.<sup>13</sup>

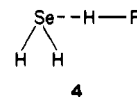
The 3799-cm<sup>-1</sup> band is assigned to the H-F stretching fundamental in the reverse complex **2** on the basis of an HF/DF ratio of 1.342 and the shift to 3791 cm<sup>-1</sup> in the analogous HF-DSD complex. The increase in intensity observed on warming indicates a stable complex in contrast to the HF-HOH<sup>4</sup> and HF-HCN<sup>11</sup> species, which decreased on annealing. The larger red-shift observed for HF-HSH indicates a much stronger complex than with HF-HOH and is consistent with the lower proton affinity for the SH<sup>-</sup> subunit (350 kcal/mol for SH<sup>-</sup> and 390 kcal/mol for OH<sup>-</sup>),<sup>14</sup> which also accounts for the increased complex stability.

The absorptions at 3714 and 3563 cm<sup>-1</sup>, which increased strongly in intensity on sample warming, are assigned to H-F stretching modes of the 1:2 complex **3** on the basis of their HF/DF ratios, 3714/2729 = 1.361 and 3563/2632 = 1.354. Clearly, the addition of the second HF molecule in **3** allows a stronger H<sub>2</sub>S-H<sub>a</sub> hydrogen bond to be formed due to the fluoride ion affinity of the H<sub>b</sub>-F submolecule. Likewise, the H<sub>b</sub>-F mode in complex **3** is reduced from the 3825-cm<sup>-1</sup> value for (HF)<sub>2</sub><sup>10</sup> due to the cooperative effect of H<sub>2</sub>S at proton H<sub>a</sub> in the complex. Therefore, the 3714-cm<sup>-1</sup> absorption is assigned to H<sub>b</sub>-F and the 3563-cm<sup>-1</sup> band to H<sub>a</sub>-F. The smaller 1-cm<sup>-1</sup> shift for H<sub>b</sub>-F to 3713 cm<sup>-1</sup> in D<sub>2</sub>S-(HF)<sub>2</sub> and larger 7-cm<sup>-1</sup> shift to 3556 cm<sup>-1</sup> for H<sub>a</sub>-F support the assignments given for these modes. The absorptions at 554 and 534 cm<sup>-1</sup> above the  $\nu_1$  doublet of **1** and at 468 and 457 cm<sup>-1</sup> below the doublet are assigned to librational modes  $\nu_1$  of the H<sub>a</sub>-F and H<sub>b</sub>-F submolecules in **3**, on the basis of appropriate changes in intensity after annealing.

The band at 3513 cm<sup>-1</sup>, which grows in strongly on warming in more concentrated H<sub>2</sub>S experiments, is assigned to the H-F stretching mode in the H<sub>2</sub>S-HF-HSH complex. Displacement of this band below the H<sub>a</sub>-F mode of complex **3** is expected due to the greater acidity of HSH relative to H<sub>b</sub>-F, which supports a slightly stronger H<sub>2</sub>S-HF hydrogen bond.

The strong product bands at 3489, 3425, 3380, 3282, and 3150 cm<sup>-1</sup>, which grew in on matrix annealing, are due to higher order complexes, most likely (H<sub>2</sub>S)(HF)<sub>x</sub>. The large displacement of these absorptions is indicative of stronger hydrogen bonding and weaker H-F bonds. The low-frequency absorptions at 575, 599, and 604 cm<sup>-1</sup>, which were observed in more concentrated experiments, are also assigned to these complexes, on the basis of their positions above the librational modes of **1** and **3**.

**H<sub>2</sub>Se + HF Assignments.** The strong absorption at 3655 cm<sup>-1</sup> is assigned to the  $\nu_3(\text{H-F})$  stretching mode of the H<sub>2</sub>Se-HF complex **4**, on the basis of an HF/DF ratio of 3655/2691 = 1.358



and the small red-shift to 3651 cm<sup>-1</sup> for D<sub>2</sub>Se-HF. The bands at 479 and 461 cm<sup>-1</sup> are assigned to the in-plane and out-of-plane librational modes  $\nu_1$  again based on large DF and small D<sub>2</sub>Se shifts. The HF/DF ratios of 479/381 = 1.257 and 461/359 = 1.284 imply asymmetry and anharmonicity in the librational potential functions. The weak broad absorption at 834 cm<sup>-1</sup> is assigned to the overtone  $2\nu_1$  of the strong 461-cm<sup>-1</sup>  $\nu_1$  mode based on the large red-shift to 820 cm<sup>-1</sup> in D<sub>2</sub>Se-HF. The weaker  $2\nu_1$  component was not observed. Anharmonicity in the librational potential function is further indicated by the  $2\nu_1/\nu_1$  ratio of 1.809.

The band at 3783 cm<sup>-1</sup> is assigned to the H-F stretching mode in the reverse complex HF-HSeH on the basis of an HF/DF ratio of 3783/2811 = 1.346. The red-shift of the HF stretching mode from isolated HF (3919 cm<sup>-1</sup>) is greater than that observed for the HF-HSH reverse complex, which is expected on the basis of the differences in intrinsic acidity of the H<sub>2</sub>Se and H<sub>2</sub>S submolecules (PA(HSe<sup>-</sup>) = 339, PA(HS<sup>-</sup>) = 350 kcal/mol).<sup>14</sup>

The absorptions at 3719 and 3595 cm<sup>-1</sup> are assigned to the H<sub>b</sub>-F and H<sub>a</sub>-F modes, respectively, of the 1:2 complex analogous to **3**, on the basis of appropriate HF/DF ratios and their proximity above and below the single  $\nu_3$  absorption of the H<sub>2</sub>Se-HF complex. The assignments for the other H<sub>2</sub>Se + HF reaction product bands, which grew in strongly on warm-up, are analogous to those given for H<sub>2</sub>S + HF with small shifts due to the differences in the intrinsic basicities or acidities of H<sub>2</sub>Se and H<sub>2</sub>S; these are collected in Table II.

**Bonding Trends.** The magnitude of the displacement of the  $\nu_3(\text{H-F})$  stretching mode from the impurity-induced HF Q-branch value of 3919 cm<sup>-1</sup> in solid argon<sup>10</sup> ( $\Delta\nu_3$ ) gives an indication of the strength of the hydrogen bond in a given complex. Stronger bases, as measured by gas-phase proton affinities, should form stronger hydrogen bonds to HF. The base molecules H<sub>2</sub>S and H<sub>2</sub>Se have proton affinities 4 and 5 kcal/mol, respectively,<sup>15</sup> higher than the base H<sub>2</sub>O whose proton affinity has been recently established as 167 ± 2 kcal/mol.<sup>15</sup> The magnitude of  $\Delta\nu_3$  shows that H<sub>2</sub>O forms a substantially stronger complex with HF than H<sub>2</sub>S and H<sub>2</sub>Se and that the H<sub>2</sub>S complex **1** is slightly stronger than the analogous H<sub>2</sub>Se complex. This trend is in agreement with ab initio calculations<sup>16</sup> and opposite to that expected from proton affinities of the bases.<sup>15</sup> This indicates that the relative stabilities of H<sub>3</sub>O<sup>+</sup> and H<sub>3</sub>S<sup>+</sup> are not good predictors of the relative stabilities of H<sub>2</sub>O-HF and H<sub>2</sub>S-HF, which may arise from limited ability of the hydrogen in HF to polarize the larger lone electron pair.

The librational modes also provide information about the complexes. The decrease in  $\nu_1$  values in the H<sub>2</sub>O-HF, H<sub>2</sub>S-HF, and H<sub>2</sub>Se-HF series demonstrates a decrease in rigidity of the complexes in this order. The  $\nu_1$  mode separation also decreases from 100 to 27 to 18 cm<sup>-1</sup> in this series of complexes, which indicates a decrease in asymmetry of the lone pair orbital forming the hydrogen bond; the more diffuse 4p orbital on Se is more nearly symmetric than the 3p orbital on S. The  $\nu_1$  mode separations for **1** and **4** are comparable to that found for the C<sub>2</sub>H<sub>4</sub>-HF  $\pi$  complex<sup>17</sup> and are consistent with the pyramidal complex structure.<sup>6,7,18</sup>

The red-shifts of  $\nu_3(\text{H-F})$  H-F stretching fundamentals observed with increasing base proton affinities usually occur with

(12) Arlinghaus, R. T.; Andrews, L., to be submitted for publication.  
 (13) Tursi, A. J.; Nixon, E. R. *J. Chem. Phys.* **1970**, *53*, 518. Barnes, A. J.; Howells, J. D. R. *Chem. Soc., Faraday Trans.* **2** **1977**, *68*, 729.  
 (14) Beauchamp, J. L. In "Interactions Between Ions and Molecules"; Ausloos, P., Ed.; Plenum Press: New York, 1975.

(15) Wolf, J. F.; Staley, R. H.; Kappel, I.; Taagepara, M.; McIver, R. T., Jr.; Beauchamp, S. L.; Taft, R. W. *J. Am. Chem. Soc.* **1977**, *99*, 5417. Collyer, S. M.; McMahon, T. B. *J. Phys. Chem.* **1983**, *87*, 909.  
 (16) Allen, L. C. *J. Am. Chem. Soc.* **1975**, *97*, 6921.  
 (17) Andrews, L.; Johnson, G. L.; Kelsall, B. J. *J. Chem. Phys.* **1982**, *76*, 5767.  
 (18) Singh, U. C.; Kollman, P. C. *J. Chem. Phys.* **1984**, *80*, 353.

an increase in  $\nu_1$  fundamentals and characterize a more rigidly bound hydrogen-bonded complex. The strengths of the  $\text{H}_2\text{S}-\text{HF}$  and  $\text{H}_2\text{Se}-\text{HF}$  hydrogen bonds are similar on the basis of almost equal values of  $\Delta\nu_1$ , but the  $30\text{-cm}^{-1}$  decrease in  $\nu_1$  modes for the  $\text{H}_2\text{Se}$  complex relative to  $\text{H}_2\text{S}$  characterizes a less rigidly bound complex. The same trend of decreasing complex rigidity for hydrogen bonds of similar strengths has been observed for the HF complexes of the increasingly heavier  $\text{CH}_3\text{Cl}$ ,  $\text{CH}_3\text{Br}$ , and  $\text{CH}_3\text{I}$  bases.<sup>19</sup> The trend of increasing stability of the reverse complexes  $\text{HF}-\text{HAH}$  for  $\text{A} = \text{O}, \text{S},$  and  $\text{Se}$  on the basis of displacement of the  $\nu(\text{H}-\text{F})$  fundamental follows the strength of the HAH acids as determined by proton affinities<sup>14</sup> of  $\text{AH}^-$  but is not in accord with calculated dimerization energies<sup>16</sup> for this series of reverse complexes. It is possible that larger basis sets will be required for more accurate calculations involving  $\text{H}_2\text{S}$  and  $\text{H}_2\text{Se}$ .

The separation between the  $\nu_s(\text{H}-\text{F})$  stretching mode of the 1:1 complexes (1) and the  $\nu(\text{H}_a-\text{F})$  stretching mode of the 1:2 complex (2) decreases in the order  $\text{H}_2\text{O}$  ( $295\text{ cm}^{-1}$ )<sup>4</sup> >  $\text{H}_2\text{S}$  ( $89\text{ cm}^{-1}$ ) >  $\text{H}_2\text{Se}$  ( $60\text{ cm}^{-1}$ ). The difference is most significant between  $\text{H}_2\text{S}-\text{HF}$  and  $\text{H}_2\text{Se}-\text{HF}$  because of the equally strong 1:1 complex hydrogen bonds of these complexes. We would expect equal displacements of the  $\text{H}_a-\text{F}$  modes due to the fluoride ion affinity of the  $\text{H}_b-\text{F}$  submolecule in a chainlike complex. The displacement

of  $\text{H}_a-\text{F}$  depends on the strength of the base- $\text{H}_a$  hydrogen bond that in turn depends on the distance between the base and the  $\text{H}_a$  atom. This implies a decrease in the polarizing strength of the proton  $\text{H}_a$  in  $\text{H}_a-\text{F}$  when confronted by the more diffuse lone pairs of the heavier bases.

### Conclusions

The cocondensation of  $\text{Ar}/\text{H}_2\text{S}$  or  $\text{Ar}/\text{H}_2\text{Se}$  with  $\text{Ar}/\text{HF}$  samples at 12 K has revealed several different hydrogen-bonded complexes. The 1:1  $\text{H}_2\text{S}-\text{HF}$  complex is characterized by a strong  $\nu_s(\text{H}-\text{F})$  stretching mode at  $3652\text{ cm}^{-1}$  and two librational modes at  $508$  and  $481\text{ cm}^{-1}$ . The  $3655\text{-cm}^{-1}$  value of  $\nu_s$  for  $\text{H}_2\text{Se}-\text{HF}$  indicates an equally strong hydrogen bond, which is expected on the basis of gas-phase proton affinities. Low  $2\nu_1/\nu_1$  ratios and decreasing librational fundamentals for  $\text{H}_2\text{S}-\text{HF}$  and  $\text{H}_2\text{Se}-\text{HF}$  indicate decreasing complex rigidity and anharmonic librational potential functions. A sharp absorption at  $3799\text{ cm}^{-1}$ , which increased on matrix annealing, characterizes a stable  $\text{HF}-\text{HSH}$  reverse complex. Several other complexes, including a 1:2  $\text{H}_2\text{S}-(\text{HF})_2$  chainlike complex and a 2:1  $\text{H}_2\text{S}-\text{H}-\text{F}-\text{HSH}$  complex, have been identified.

**Acknowledgment.** We gratefully acknowledge support from NSF Grant CHE 82-17749 and assistance from our inorganic colleagues on the synthesis of hydrogen selenide.

**Registry No.**  $\text{H}_2\text{S}$ , 7783-06-4;  $\text{H}_2\text{Se}$ , 7783-07-5;  $\text{HF}$ , 7664-39-3.

(19) Arlinghaus, R. T.; Andrews, L. *J. Phys. Chem.* **1984**, *88*, 4032.

Contribution from the Department of Chemistry, Faculty of Science, Nara Women's University, Nara 630, Japan

## Light-Induced Ligand-Substitution Reactions. Reaction between the Chloropentaamminecobalt(III) Ion and Ethylenediaminetetraacetate by Irradiation with Visible Light of Aqueous Solutions Containing the Tris(2,2'-bipyridine)ruthenium(II) Ion

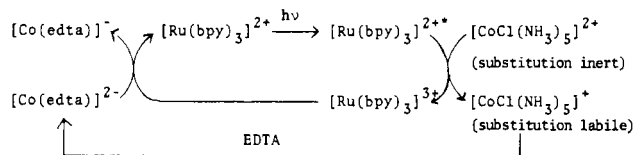
MASARU KIMURA,\* MARI YAMASHITA, and SUZUKO NISHIDA

Received July 5, 1984

The ligand-substitution reaction between the chloropentaamminecobalt(III) ion,  $[\text{CoCl}(\text{NH}_3)_5]^{2+}$ , and ethylenediaminetetraacetate, which denotes all the forms of edta, i.e.,  $\text{edta}^{4-}$ ,  $\text{Hedta}^{3-}$ ,  $\text{H}_2\text{edta}^{2-}$ , etc., was induced by irradiation with visible light of aqueous solutions of acetate buffer (pH 4.75) containing the tris(2,2'-bipyridine)ruthenium(II) ion,  $[\text{Ru}(\text{bpy})_3]^{2+}$ , and  $[\text{Co}(\text{edta})]^-$  was efficiently produced, where  $[\text{Ru}(\text{bpy})_3]^{2+}$  acts as an inductor and as a photocatalyst. The ligand-substitution reaction constitutes a chain reaction containing a cycle of  $[\text{Ru}(\text{bpy})_3]^{2+}$  and  $[\text{Ru}(\text{bpy})_3]^{3+}$ , where the reaction is initiated by the reaction between the photoexcited complex  $[\text{Ru}(\text{bpy})_3]^{2+*}$  and  $[\text{CoCl}(\text{NH}_3)_5]^{2+}$ . The rate of the formation of  $[\text{Co}(\text{edta})]^-$  is described essentially by a rate law of  $d[\text{Co}(\text{edta})^-]/dt = I_a \Phi k_q [[\text{CoCl}(\text{NH}_3)_5]^{2+}] / \{k_0 + k_q [[\text{CoCl}(\text{NH}_3)_5]^{2+}]\}$ , where  $I_a \Phi$  corresponds to the formation rate of  $[\text{Ru}(\text{bpy})_3]^{2+*}$ ,  $k_q$  is the quenching rate constant of  $[\text{Ru}(\text{bpy})_3]^{2+*}$  by  $[\text{CoCl}(\text{NH}_3)_5]^{2+}$ , and  $k_0$  is the quenching constant of  $[\text{Ru}(\text{bpy})_3]^{2+*}$  due to the light emission and to the thermal energy loss. The reaction mechanisms and the rate law are verified by the results obtained. The bimolecular quenching constants  $k_q$  are determined by means of the kinetic experiments for the light-induced ligand-substitution reaction and are compared to the  $k_q$  values that are obtained by measurements of luminescence of  $[\text{Ru}(\text{bpy})_3]^{2+*}$ .

Although the abbreviation EDTA is generally for ethylenediaminetetraacetic acid, i.e.,  $\text{H}_4\text{edta}$ , we use, throughout this paper, EDTA for all the forms of  $\text{H}_4\text{edta}$ ,  $\text{H}_3\text{edta}^-$ ,  $\text{H}_2\text{edta}^{2-}$ ,  $\text{Hedta}^{3-}$ , and  $\text{edta}^{4-}$ . It is known that the oxidative quenching of the photoexcited ruthenium(II) complex  $[\text{Ru}(\text{bpy})_3]^{2+*}$  (bpy = 2,2'-bipyridine) by  $[\text{CoCl}(\text{NH}_3)_5]^{2+}$  produces  $[\text{Ru}(\text{bpy})_3]^{3+}$  and  $[\text{CoCl}(\text{NH}_3)_5]^{2+}$ , and that the latter species dissociates rapidly to  $\text{Co}^{2+}_{\text{aq}}$ ,  $\text{Cl}^-$ , and  $\text{NH}_3$  (or  $\text{NH}_4^+$ ),<sup>1-3</sup> in which  $\text{Co}^{2+}_{\text{aq}}$  could form  $[\text{Co}(\text{edta})]^{2-}$  rapidly in an aqueous solution with acetate buffer (pH 4.75) if EDTA is present in the reaction mixture. The  $[\text{Ru}(\text{bpy})_3]^{3+}$  ion is so a strong oxidant as to oxidize  $[\text{Co}(\text{edta})]^{2-}$  to  $[\text{Co}(\text{edta})]^-$ . Therefore, we could design an experiment for the light-induced substitution reaction between  $[\text{CoCl}(\text{NH}_3)_5]^{2+}$  and EDTA by employing  $[\text{Ru}(\text{bpy})_3]^{2+}$  as a catalyst. This reaction can be briefly described as shown in Scheme I. In this paper

### Scheme I



we demonstrate that the proposed scheme operates well in an acetate buffer solution of pH 4.75, and the operation mechanisms are discussed.

### Experimental Section

**Chemicals.**  $[\text{Ru}(\text{bpy})_3]\text{Cl}_2 \cdot 6\text{H}_2\text{O}$  was prepared as described in the literature<sup>4</sup> and recrystallized twice.  $[\text{CoCl}(\text{NH}_3)_5]\text{Cl}_2$  was prepared as described in the literature<sup>5</sup> and recrystallized twice. Disodium di-

(1) Neumann-Spallart, M.; Kalyanasundaram, K. *Ber. Bunsenges. Phys. Chem.* **1981**, *85*, 704.  
 (2) Kalyanasundaram, K.; Gräzel, M. *Helv. Chim. Acta* **1980**, *63*, 478.  
 (3) Gafney, H. D.; Adamson, A. W. *J. Am. Chem. Soc.* **1972**, *94*, 8238.

(4) Tachibana, T.; Nakahara, M.; Shibata, M., Eds. "Shin Jikken-Kagaku Koza 8"; Japan Chemical Society: Maruzen, 1975; p 1475. Palmer, R. A.; Piper, T. S. *Inorg. Chem.* **1966**, *5*, 964. Fujita, I.; Kobayashi, H. *Ber. Bunsenges. Phys. Chem.* **1972**, *76*, 115.